Arabian Journal for Science and Engineering (2022) 47:5033–5051
https://doi.org/10.1007/s13369-021-06426-5

RESEARCH ARTICLE-CIVIL ENGINEERING

Structural Optimization Behavior of Green Concrete Members

Ilyas Saribas[1]

Received: 16 September 2021 / Accepted: 18 November 2021 / Published online: 9 January 2022

Abstract

The recycling process of construction and demolition waste, which started with brick pieces and brick dust used in the production of binder thousands of years ago, gained momentum after the second world war. Nowadays, the recycling activities of waste materials are sustained much more effectively by developing technology, machinery, and equipment. The obtained material by recycling waste concrete is called recycled concrete aggregate. And it has been stated in many experimental, analytical studies in the literature and more than one international material code that the recycled concrete aggregate, which meets specific material criteria, is an alternative to natural aggregate. This current study is carried out to give a different perspective and contribute to the literature on a not researched topic. Therefore, within the scope of this recent study, the structural topology optimization of structural members was performed by the isoline topology design method. The concrete properties of these members are considered with the natural concrete and the recycled aggregate concrete with four different recycled concrete aggregate ratios (25%, 50%, 75%, 100%). Besides, the structural topology optimization was performed by considering multi-material and single-material properties under similar loading conditions. As a result of the optimization process, the quantified optimization shapes indicated that the structural optimization behavior of multi-material structural members exhibits different optimization behavior depending on the recycled concrete aggregate ratios. However, considering the single-material situation, it is observed that the structural optimization behavior of structural members is similar for all concrete types. Finally, comparing the optimization shapes of natural concrete members with the recycled aggregate concrete members indicated that the structural topology optimization process applied to structural members incorporating natural concrete is also valid for recycled aggregate concrete members. In addition, a brief life cycle assessment of waste concrete was also carried out in this comprehensive study to emphasize the importance of recycling activities.

Keywords Column · Corbel · Isolines topology design · Natural aggregate · Optimization · Recycled aggregate · Recycled aggregate concrete · Reinforced concrete · Structure

List of symbols

A_{stotal}	The total area of main reinforcement
A_{sw}	The area of web reinforcement
a	The distance between the load application point and the RC column edge face
b_w	The web width of member
d	The effective depth
E_c	The modulus of elasticity of concrete
E_s	The modulus of elasticity of steel
f_c	The concrete compressive strength
f_{cu}	The ultimate concrete compressive strength
f_{ck}	The characteristic concrete compressive strength
f_{ct}	The concrete uniaxial tensile strength
f_{sy}	The yield strength of reinforcing bar
h	The depth of member cross-section
i	The recycled concrete aggregate coefficient
s	The recycled concrete aggregate coefficient
ε_{co}	The strain value corresponding to the maximum concrete compressive strength
ε_{cu}	The ultimate concrete compressive strain
P_d	The applied load
σ_x, σ_y, τ_{xy}	The normal stresses and shear stress
V_{cr}	The crack shear strength of concrete
V_c	The shear strength of concrete
V_{rmax}	The maximum shear strength

✉ Ilyas Saribas
isaribas@atu.edu.tr

[1] Civil Engineering Department, Faculty of Engineering, Adana Alparslan Türkeş Science and Technology University, 01250 Sarıçam, Adana, Turkey

k	The constant fix ratio
ε_s*, ε_C*	The tensile and compressive maximum strains
ρ_s, ρ_C	The unit weight of tension and compressive material
k_1	The constant fix ratio between stresses
σ_s*, σ_C*	The tensile and compressive maximum stresses
σ^i	The criterion value at the i node
σ^e	The criterion value at each element
$\sigma_e{}^i$	The nodal criterion value for each element
N_e	The number of elements
V_e	The volume for each element
N_i	The number of nodes
σ	The design criterion like Von Mises stress (σ_{vM})
ξ^e	The design fraction inside the element
FG_R	The Fixed Grid ratio
K_I, K_O, K_B	The element stiffness matrices for an element inside, outside and boundary
K^e	The element stiffness matrix
Vi	The design volume in the ith iteration
V_0	The initial volume
V_f	The final volume of the optimized structure
n_i	The total number of iterations

1 Introduction

The construction industry is one of the leading industries that play a critical role in developing and developed countries. The primary material of the construction industry is concrete. With the developing technology, concrete finds many usage areas in the world [1–3]. Nowadays, most of the structures are constructed from concrete with conventional methods. However, concrete is not material with eternal life. Therefore, it is essential to eliminate the waste concrete that has completed their life. In addition, regional and global wars, natural disasters (especially earthquakes), restoration works, urban transformation programs can be stated as the factors that cause concrete to turn into waste materials [4, 5]. The waste concrete resulting from these effects through the 4Rs rule: Reduce, Recycle, Reuse, and Resell or Rebuy have been eliminated very quickly and effectively from the beginning of the 2000s with increasing knowledge, experience, machinery, and equipment. As a result of recycling and reuse (waste treatment) activities, millions of tons of waste concrete are eliminated in European countries by contributing to countries' society, environment, and economy (Fig. 1).

Recycled concrete aggregates (RCA) are obtained from the recycling activities of construction and demolition waste concrete. With increasing awareness of RCA in the production of new structures, the number and scope of related studies have reached a significant level in recent years [1–3, 6, 7]. Within the scope of these studies, while previously only RCA and the characteristics of recycled aggregate concrete (RAC) produced with RCA have been investigated [3, 6–8], different performance values of significant structural members with different scales containing RAC are now being investigated [3–11]. Furthermore, many international documents are stating that these RCA and RAC are alternative products to natural aggregate (NA) and Natural aggregate concrete (NAC) [3, 7, 11].

When designing reinforced concrete (RC) members, these members are generally divided into two regions. These are B and D regions [12–15]. Region B is where Beam and Bernoulli's hypotheses are valid, and region D is called disturbed or discontinuous [12–15]. For the D regions, the stress distribution is non-linear, and Bernoulli's hypotheses are not valid. Therefore, the design and analysis of B-regions of structural members such as beams, columns, slabs constructed by NAC or RAC can be designed and analyzed according to conventional sectional methods [16, 17]. However, it is not appropriate to design and analyze the members with D-region (with small span-to-depth ratio structural members) using conventional sectional methods [18, 19]. For instance, short corbels generally grouped into double short corbels (DSC) or single short corbels (SSC) are structural members that have a discontinuity in both load and geometry and transfer the loads on them to RC columns and RC shear walls. Therefore, it is clear that these members should not be designed according to the Bernoulli hypotheses that the plane section remains plane after loading, and the transverse clamping stresses are neglected as in conventional RC theory [18–21]. It should also be noted that these members are designed region-based rather than section-based, like deep beams [22, 23]. Furthermore, the main reinforcement details resist flexure and shear effects in these members, while the secondary controls the crack widths [23].

There are some methods in the literature for the design of structural members with D regions. One of them is the strut and tie method (STM). The STM is a method that considers the truss analogy method first proposed by Ritter [24] and Mörsch [25, 26]. This method was later modified by some researchers [27–30]. Furthermore, this method is currently used and recommended by different international structural documents to design D regions [12–15]. Although the STM is considered a simple method for designing D regions of structural members, the main handicap of this method is the difficulty of iteration for the designing of these members [31, 32].

When designing structures, the main target of structural engineers is always to design structural systems, both economically and structurally safe [33]. One of the developed methods for responding to these demands of structural engineers is the structural optimization method. This computational design method makes it possible to find optimized

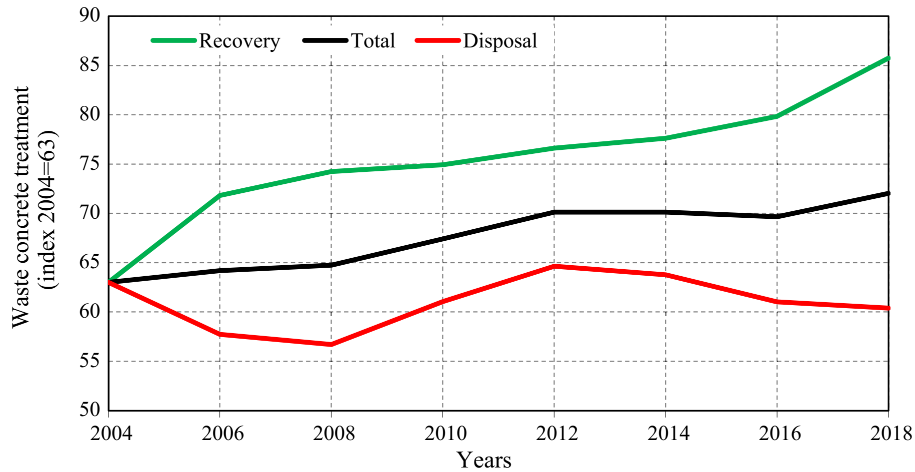

Fig. 1 Treatment of waste concrete (index 2004 = 63) [5]

structures through numerical analysis. There have been three different types of structural optimization methods in the literature: size, shape, and topology optimization used by many researchers for structural optimization, which eliminates several difficulties in STM. While many structural optimization methods are in the literature, the topology optimization method is the most general form of structural optimization. Because topology optimization aims to design the structural members without manipulating the size and shape of these members' components, this method provides a numerical iterative procedure that automatically redistributes the material within a reference design surface under appropriate boundary conditions to optimize the structural members. Therefore, the topology optimization method has gained significant popularity since 1980. And this method has been used by many researchers for structural optimization [34–41]. Besides, there are some digital topology optimization methods for designing the structural members, such as computer-aided design, formation, generative, performance, and integrated compound models.

On the other hand, while there are many methods for implementing topology optimization effectively for structural optimization, the mathematical-based procedures: homogenization, solid isotropic microstructure with penalization, level set method, and growth method for truss structures [42–45], and the heuristic-based procedures: sequential element rejection and admission, fully stress design, computer-aided optimization, soft kill option, evolutionary structural optimization, bidirectional evolutionary structural optimization, and isoline/isosurface topology design are widely used [45]. In this study, the isoline/isosurface topology optimization (ITD) method was used. The ITD method is a heuristic-based digital performance model since the structural members are optimized according to the desired performance. Although the material removal and addition procedure play a critical role in finding the optimal design, the ITD method designs the structural members using the isosurfaces and the von Mises stress option via integrated procedure up to the desired volume fraction. It should also be noted that while the ITD method has been used for many years to design structural members incorporating NAC, according to the author's best knowledge, this method has not yet been used for structural members containing RAC. And this is the first time that the structural topology optimization results of structural members incorporating RCA are reported in detail in a paper. Therefore, there is a significant research gap in the literature on this research area. And this study contributes to the literature to address the scarcity of technical information about this topic. This comprehensive study investigates the structural topology optimization behaviors of the multi-material and single-material RAC members (RC single short corbels and columns) assumed to be produced with 25%, 50%, 75%, and 100% RCA. And the obtained structural topology optimization results of RAC members are given in comparison with the optimization results of the NAC member. Finally, a brief life cycle assessment of waste concrete was also carried out in this comprehensive study to emphasize the importance of recycling activities.

2 Materials and Methods

2.1 Material Properties of Structural Members

The necessary material properties of NAC and RAC to be considered within the scope of the study were obtained from the modified Hognestad [46] model proposed by Saribas [47]. Not to mention the fact that before any experimental or analytical studies on RCA, it is critical to determine the characteristics of RCA. After determining the characteristic properties of RCA, it is another essential point to know the stress–strain relationship of RAC. Knowing the stress–strain relationship of concrete contributes to understanding the behavior of the structural member. In this study, the stress–s-

Table 1 i and s coefficients according to RCA ratio

Mixture	RCA ratio (%)	i coefficient	s coefficient
NAC	0	1.00	1.00
RAC25	25	0.95	0.95
RAC50	50	0.90	0.80
RAC75	75	0.85	0.75
RAC100	100	0.80	0.70

train relationship of RAC was determined for different ratios of RCA. Concrete compressive strength (f_c) in the stress–strain relationship is defined as in Eq. (1). The value of the s coefficient in this equation changes according to Table 1, depending on the RCA ratio. The modulus of elasticity (E_c) in the same relationship is defined as in Eq. (2). And the i coefficient in this equation changes according to Table 1, depending on the RCA ratio. For instance, 50% by weight of RCA is used in new concrete, s and i coefficients in Eqs. 1 and 2 are considered 0.80 and 0.90, respectively.

It should also be mentioned that the ascending branch of the stress–strain relationship of RAC is regarded with a second-order parabola as in the Hognestad [46] model (Eq. (4)). In this curve, the axial strain (ε_{co}) corresponding to the maximum concrete compressive strength is considered by Eq. (3). And the ultimate concrete compressive strength (f_{cu}) is defined as in Eq. (5). In addition, the maximum ultimate strain (ε_{cu}) is regarded as 0.0040. All parameters of the stress–strain relationship of RAC are valid for normal concrete strength.

$$f_c = s \times 0.85 f_{ck} \tag{1}$$

$$E_c = 12680 + i \times 460 f_c \tag{2}$$

$$\varepsilon_{co} = \frac{2 f_c}{E_c} \tag{3}$$

$$\sigma_c = f_c \left(\frac{2\varepsilon_c}{\varepsilon_{co}} - \left(\frac{\varepsilon_c}{\varepsilon_{co}} \right)^2 \right) \tag{4}$$

$$f_{cu} = 0.85 f_c \tag{5}$$

In this current study, f_{ck} is considered as 35 MPa. The stress–strain relationships obtained according to this value are given in Fig. 2. Concrete parameters of NAC and RAC members obtained from the modified model are shown in Table 2. In these relationships (Fig. 2), NAC, RAC25, RAC50, RAC75, and RAC100 represent the stress–strain curves obtained by the modified Hognestad [46] model of the concrete produced with NA and different RCA ratios (25%, 50%, 75% and 100% by weight of RCA). As seen in Fig. 2 and Table 2, as the RCA ratio in RAC increases, both the f_c and the E_c decrease. While the f_c and E_c of NAC are negligibly higher than the RAC25, these two parameters of NAC are substantially higher than those of RAC50, RAC75, and RAC100. It should also be mentioned that although RCA is used at different ratios in new concrete, the stress–strain curve of RAC is not different from the NAC stress–strain curve [3, 6, 47–50].

Furthermore, the unit weight values of the NAC and RACs are given in Table 2. As seen in this table, different unit weights were considered for NAC and RAC. It is mentioned in the literature that the unit weight of RAC is generally lower than that of NAC [3, 7, 11]. Therefore, the unit weight values of 2400 kg/m^3 and 2300 kg/m^3 were used for NAC and RAC (RAC25, RAC50, RAC75, RAC100). On the other hand, the B420C, which was defined in the Turkish Seismic Design Code (TSDC) [51] as the reinforcing steel, has been considered as a reinforcing bar. The stress–strain curve of this reinforcing bar is given in Fig. 3, and yielding stress (f_{sy}), modulus of elasticity (E_s), and unit weight (ρ_s) of this reinforcing bar are given in Table 2.

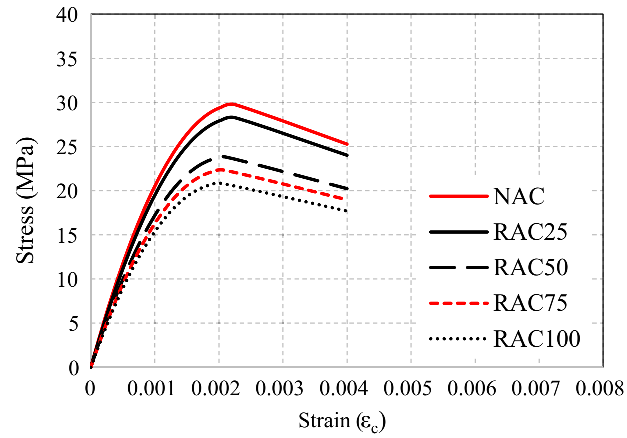

Fig. 2 Stress–strain relationships of NAC and RAC

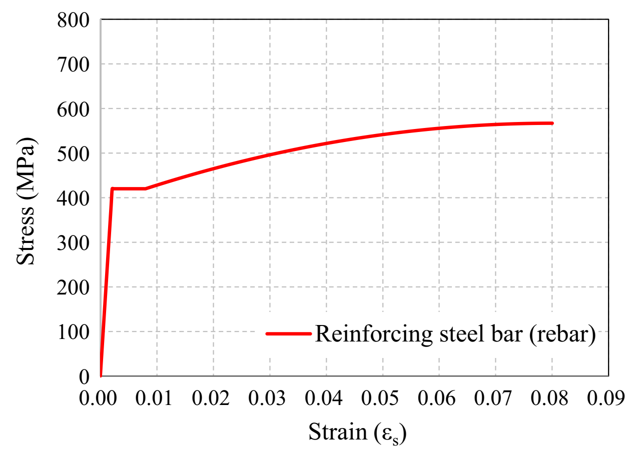

Fig. 3 Stress–strain relationships of the deformed reinforcing bars

Table 2 Material properties of structural members

Specimens	f_c (MPa)	f_{cu} (MPa)	E_c (MPa)	ρ_c (kg/m^3)	ε_{co}	f_{sy} (MPa)	E_s (GPa)	ρ_s (kg/m^3)	k_I	k
NAC	30.0	25.5	26,365	2400	0.00228	420	200	7850	4.98	0.66
RAC25	28.3	24.1	25,030	2300	0.00226	420	200	7850	5.22	0.65
RAC50	23.8	20.2	22,533	2300	0.00211	420	200	7850	5.50	0.62
RAC75	22.3	19.0	21,404	2300	0.00208	420	200	7850	5.65	0.60
RAC100	20.8	17.7	20,344	2300	0.00205	420	200	7850	5.79	0.59

2.2 Background of Isolines Topology Optimization Method

While the engineer's intuition and experience are at the forefront for structural design, this situation has changed with the topology optimization method. Although there are many methods for structural optimization of structural members, these methods can be divided into two groups. The first is mathematical-based [42–45], and the other is heuristic-based [45]. In this comprehensive study, the ITD method (via liteITD), an iterative redistribution algorithm, was used for the structural topology optimization of NAC and RAC members. The redistribution procedures of the ITD method compose of four parts. First of all, the design criterion distribution obtains. Secondly, the Minimum Criterion Level (MCL), as shown in Fig. 4, is related to the new structural boundary determines. Furthermore, the MCL is determined by Eq. (6) for each iteration. Thirdly, all regions of the design field remove. Finally, this design modification requires reevaluating the remaining structure to recalculate the design criterion distribution [45, 52–56].

$$V_i = V_o + (V_f - V_o)\frac{i}{n_i} \tag{6}$$

In Eq. 6, V_i is the design volume in the ith iteration, V_0 is the initial volume, V_f is the final volume of the optimized structure, and n_i is the total number of iterations.

The matrix is given in Eq. (7) is used to calculate the structural members' element stiffness matrix (K_e). K_I, K_O, and K_B are the stiffness matrices for an element inside, outside, and on the boundary. ξ^e is the design fraction inside the element, FG_R is the Fixed Grid ratio, commonly set in the range of 10^{-6} to 10^{-4} [45, 52–56].

$$K^e = \begin{cases} K_I & \text{if } \xi^e = 1.0 \\ K_o = K_I \times FG_R & \text{if } \xi^e = 0 \\ K_B = K_I\xi^e + K_o(1 - \xi e) & \text{if } 0 < \xi^e < 1.0 \end{cases} \tag{7}$$

The criterion value (σ^i) at the i node and the criterion value (σ^e) at each element (e) are considered by Eqs. 8 and 9, respectively. In these equations, ${\sigma_e}^i$ is the nodal criterion value of each component, N_e is the number of elements, V_e is the volume of each element, N_i is the number of nodes. Furthermore, the design criterion (σ) like Von Mises stress (σ_{vM}) is considered by Eq. 10. In which σ_x, σ_y, and τ_{xy} are the normal stresses and shear stress, respectively [45, 52–56].

$$\sigma_i = \frac{\sum_{e=1}^{N_e} \sigma_e^i \times V_e}{\sum_{e=1}^{N_e} V_e} \tag{8}$$

$$\sigma^e = \frac{\sum_{e=1}^{N_i} \sigma^i}{N_i} \tag{9}$$

$$\sigma = \sigma_{vM} = \sqrt{\sigma_x^2 + \sigma_y^2 - \sigma_x\sigma_y + 3\tau_{xy}^2} \tag{10}$$

The interaction of an isoline with a triangular cell is given in Fig. 5. The values (1) and (0) at the corner points of this triangular cell indicate that the criterion values are higher and less than that of the MCL, respectively (Fig. 5a, d). When the values of this triangular cell at the corner point are (0) and (1) or (1) and (0), the MCL isoline intersects with these edges (Fig. 5b, c). It should also be noted that the structural boundary changes when the MCL is changed, and this modification affects the criterion distribution. Hence, before the next iteration begins, an iterative process of reanalysis and material redistribution is performed until the change in field volume, subsequent limit adjustments are less than that of the minimum volume change limit (1%) (Eq. 11) [45, 52–56].

$$\Delta V(\%) = \left[\frac{V_i}{V_{i-1}} - 1\right] \times 100 \tag{11}$$

2.3 Optimization Algorithm of Isoline Topology Design Method

In this study, the ITD algorithms consisting of 11 steps are performed as in Fig. 6. As seen in this figure, firstly, define the structural member such as design and non-design fields, the total number of materials, material properties for each material, load, and support conditions. Secondly, define the finite element mesh properties. Thirdly, define the isoline topology design parameters such as a design criterion, volume control weighting factor, final design volume, total number of iterations, and minimum volume change limit. Fourthly, perform

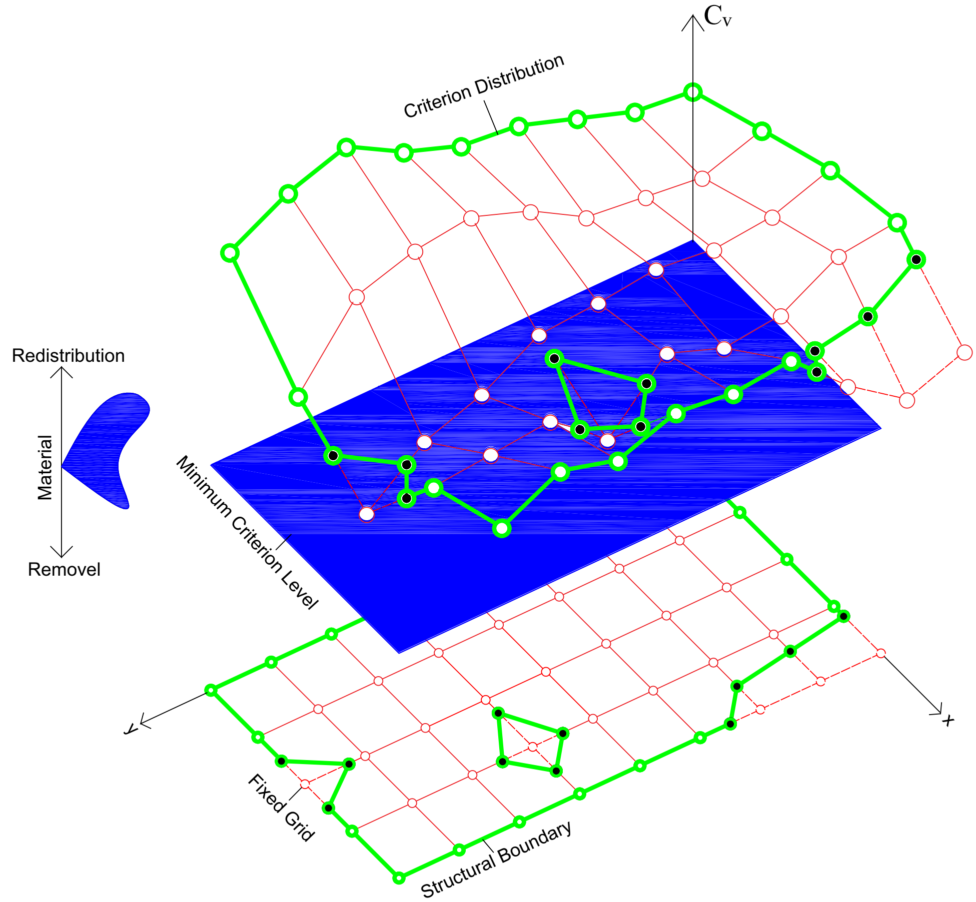

Fig. 4 The structural boundary is defined by the intersection of the minimum criterion level (MCL) with the criterion distribution [45]

a fixed grid finite element analysis. Fifthly, determine the target volume for every material type. Sixth, calculate the MCL value for every material type. Seventhly, extract the boundary of the structural element and distribute the different materials. Eighth, when the percentage volume change is greater than the minimum limit of volume change, go to step nine; otherwise, go to step ten. Perform a fixed grid finite element analysis of the design domain and go to step seven. Tenth, when the total number of iterations has been reached, go to step eleven, otherwise update the design volume, increment the iteration number by one and go to step four. Eleventh, finish the design process [45, 52–56].

2.4 The Optimality Criterion for Structural Optimization of Structural Members

Equations (12) and (13) proposed by Dewhurst [57] were used for the optimality criterion of the structural optimization design of structural members. According to this relation, when the structural members have a constant fixed strain ratio, an optimal layout of maximum stiffness-minimum volume/weight is obtained [45, 52–57]. As stated before, when the material characteristic of a structural element to be designed is known, the optimization analysis of this element or structure is carried out quickly and realistically. Thus, the stresses in the relevant area are calculated clearly during the optimization process, and all negative stresses are expanded with the coefficient k (Eq. 12). Eventually, these stress fields are then used for optimization. It should also be mentioned that depending on the analysis method; it may be more appropriate to study with stresses rather than strains. Therefore, when the strain-dependent equation (Eq. 12) is converted to stress-dependent using the modulus of elasticities, the coefficient k_1 is obtained (Eq. 13) [45, 52–57].

$$k = \frac{\varepsilon_s^*}{\varepsilon_c^*} = \left[\frac{\rho_s E_c}{\rho_c E_s}\right]^{0.5} \tag{12}$$

$$k_1 = \frac{\sigma_s^*}{\sigma_c^*} = \left[\frac{\rho_s E_s}{\rho_c E_c}\right]^{0.5} \tag{13}$$

In which k is the constant fix ratio between strains in the optimum structure, $\varepsilon_s{}^*$ and $\varepsilon_c{}^*$ are tensile and compressive maximum strains defining optimal structure layouts, E_s and E_c are the modulus of elasticities tensile and compressive members, ρ_s and ρ_c are mass, weight, or cost per unit volume of tension and compressive members, k_1 is the constant fix

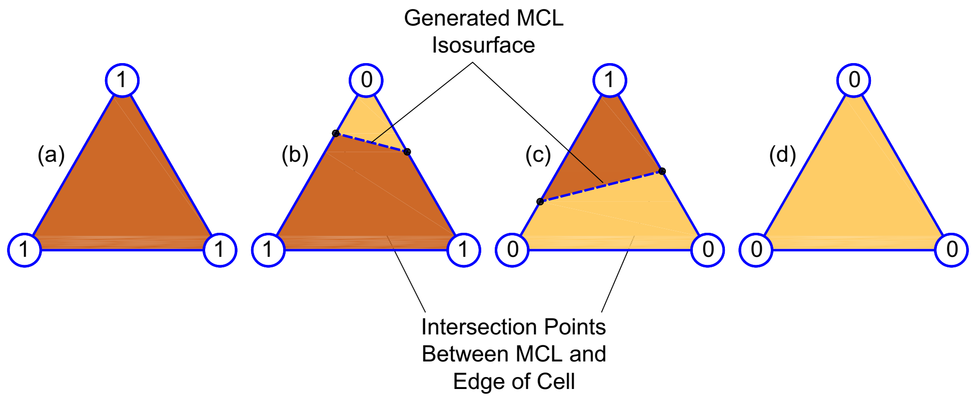

Fig. 5 The marching triangles (MT) algorithm at four different topological states [45]

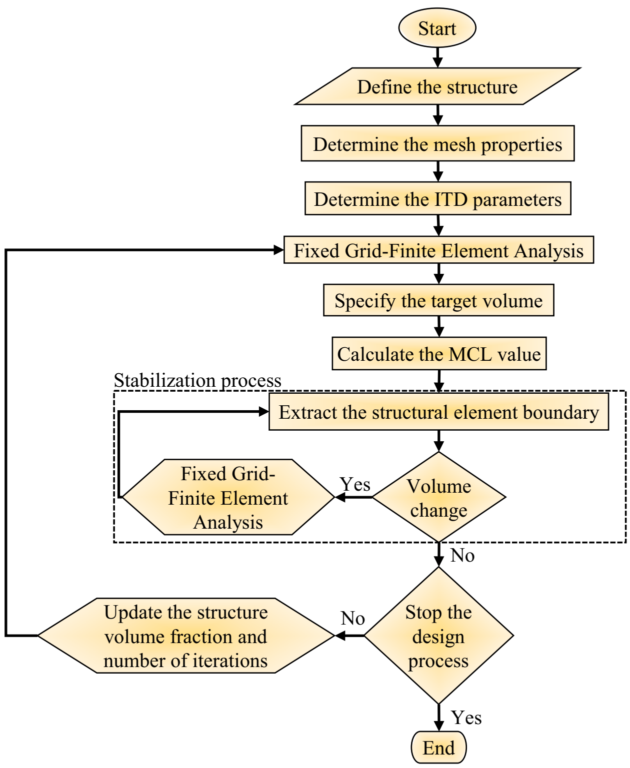

Fig. 6 Flowchart of the ITD algorithm [45]

ratio between stresses in the optimum structure, and $\sigma_s{}^*$ and $\sigma_c{}^*$ are tensile and compressive maximum stresses in the optimized structure.

3 Structural Parameters of NAC and RAC Members

When the distance between the load application point and the RC column edge face (a) is less than the height of the beam (d), these structural members are called short corbels (a/d ratio between 0.5 and 1.0). As stated before, single short corbels have discontinuities both in loading and geometrically [19, 54]. Therefore, they are not suitable to be designed according to the conventional RC theory. In this comprehensive study, the structural optimization of single short corbels and columns was performed using the ITD method. It should be noted that the type of used finite elements was the four-node plane stress quadrilateral element with four Gauss integration points. The dimension, boundary, and loading conditions of these members (dimensions in meter) are seen in Fig. 7. This figure shows that the cross-sections of columns and corbels are 600 × 400 mm and 400 × 600 mm, respectively. Furthermore, it is seen in this figure that NAC, RAC25, RAC50, RAC75, and RAC100 represent the structural members incorporating NA and different RCA ratios (25%, 50%, 75% and 100% by weight of RCA).

Furthermore, whether the dimensions of the single short corbels were sufficient or not was checked according to TS500 [58] (Table 3). And the equations suggested by ACI 318 [12] were used for the RC design of these members. The calculated data for both the dimension control and the RC design is presented in Table 3. In addition, the typical reinforcing cage of corbels is seen in Fig. 8. As seen in Table 3, the dimensions of these corbels are more than sufficient for the applied load condition. Besides, the columns are considered as fixed support at both ends. As seen in Figs. 7 and Fig. 9b, the concentrated load (500 kN) is applied on the corbels 450 mm from the column face. And these members were divided using the square finite element meshes with 15 × 15 mm (Fig. 9a).

On the other hand, the axial load-moment interaction relationships of the RC columns were obtained through a fiber-analysis approach using the XTRACT 3.0.8 [59] computer program. In this axial load-moment analysis, the stress–strain relationship of concrete in compression was modeled considering the modified Hognestad Model [46] (Fig. 2). Furthermore, the behavior of confined concrete (core concrete with stirrup confined) was considered by Mander Model [60] based on the characteristics of the transverse reinforcement, dimensions of the cross-section, and unconfined concrete features. Steel reinforcing bars in tension were

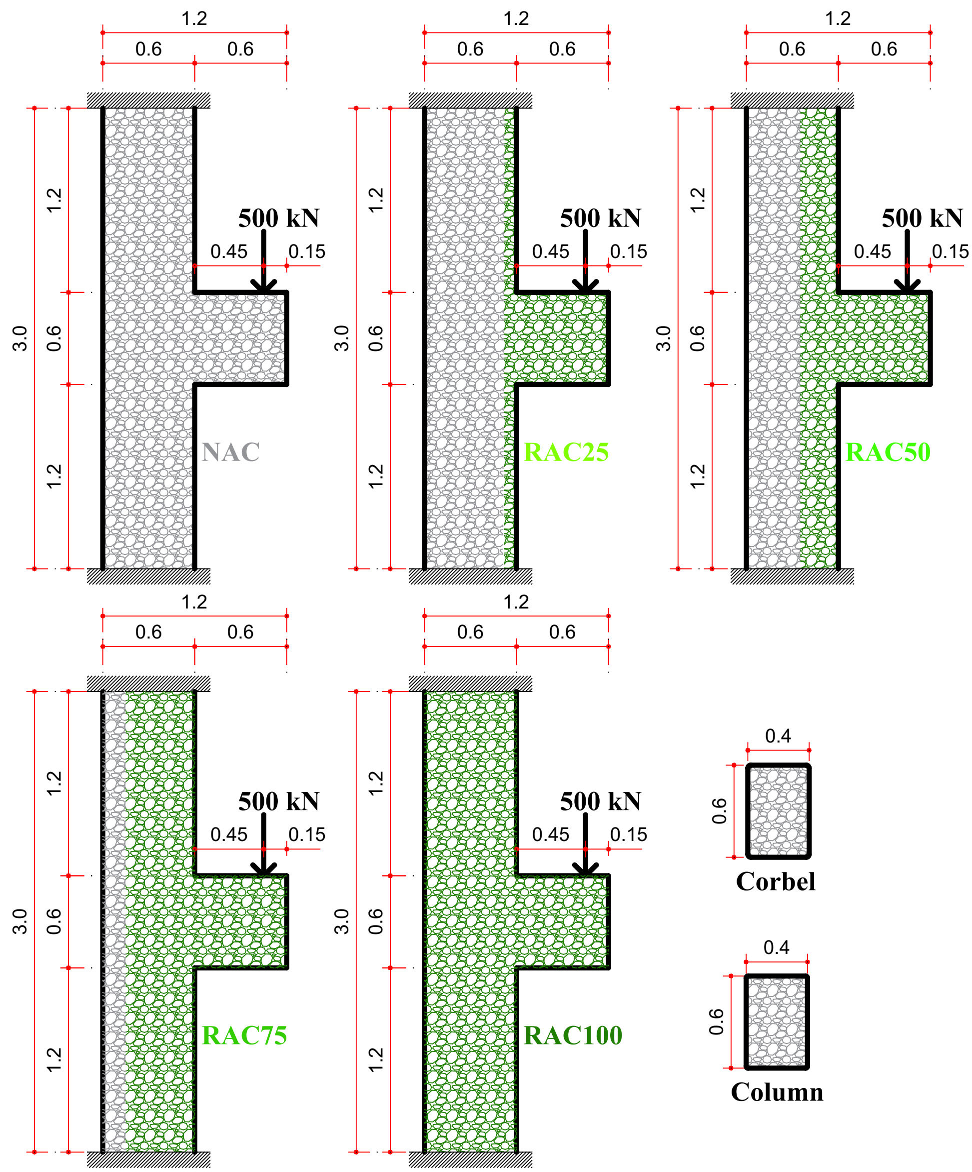

Fig. 7 Dimension, boundary, and loading conditions of the single short corbels and columns (dimensions in meter)

Table 3 Reinforced concrete design of single short corbels

Specimens	b_w (mm)	h (mm)	d' (mm)	d (mm)	f_c (MPa)	f_{ct} (MPa)	P_d (kN)	V_{cr} (kN)	V_c (kN)	V_{rmax} (kN)	$b_w \times h$	$A_{s,total}$	A_{sw}
NAC	400	600	50	550	30.0	1.92	500	274	219	1452	√	5ϕ20	4ϕ12
RAC25	400	600	50	550	28.3	1.86	500	266	213	1370	√	5ϕ20	4ϕ12
RAC50	400	600	50	550	23.8	1.71	500	244	195	1152	√	5ϕ20	4ϕ12
RAC75	400	600	50	550	22.3	1.65	500	236	189	1079	√	5ϕ20	4ϕ12
RAC100	400	600	50	550	20.8	1.60	500	228	183	1007	√	5ϕ20	4ϕ12

assumed to behave in an elastic–plastic manner with strain hardening based on the B420C rebar (Fig. 3). The geometric ratio of longitudinal reinforcement is 1.27%. And the thickness of the concrete cover is 40 mm. In addition, the number of fibers of RC columns cross-section is 570 (Fig. 10a). The obtained axial load-moment relationships of NAC and RAC columns (NAC_col, RAC25_col, RAC50_col, RAC75_col, and RAC100_col represent the columns incorporating NA and different RCA ratios: 25%, 50%, 75% and 100% by weight of RCA) are presented in Fig. 10b. Reinforced con-

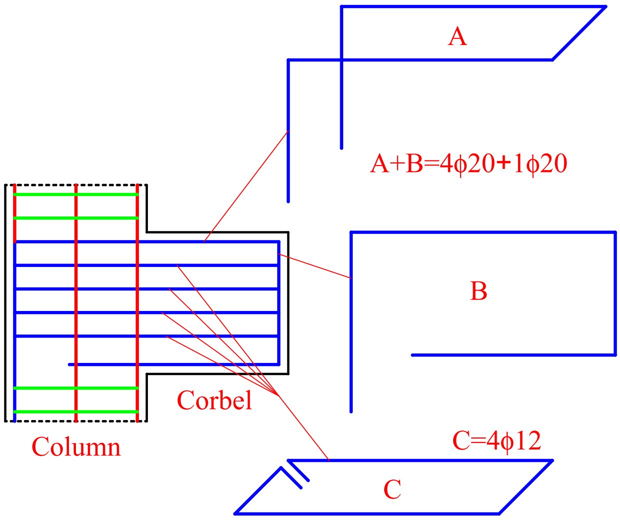

Fig. 8 Typical reinforcing cage of single short corbel (see Table 3)

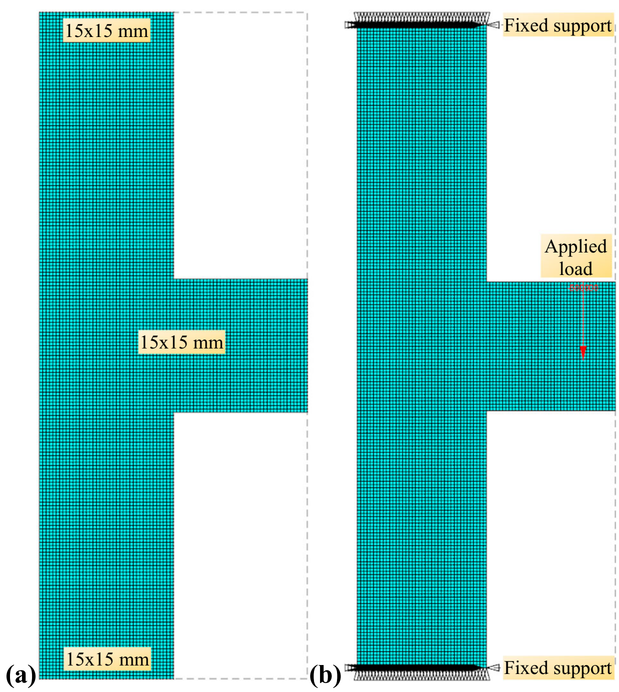

Fig. 9 Design properties of corbels and columns; **a** mesh properties, **b** ready specimen for analysis

crete columns are often subjected to axial loads and bending moment effects in extreme conditions (earthquake, impact effects, etc.) to shear effects. Therefore, the axial load-moment relationships of RC columns are vital. It is seen in this Fig. 10b that while the axial load-moment carrying capacities of NAC_col and RAC25_col columns are approximately similar, and the axial load-moment carrying capacities of the columns decrease as the RCA ratio in the new concrete increases. It should also be noted that the reduction in the columns' axial load and moment capacities is similar.

4 Optimization Results and Discussions

Structural topology optimization results of multi-materials members (reinforced concrete members) obtained by performing the ITD methods are presented in Fig. 11. It should also be stated that these optimization results were obtained by considering the 50 iterations, 30% objective volume fraction, and 2% minimum volume change. The red and blue fields in this figure represent the tension and compression regions, respectively. It is seen in Fig. 11 that the structural topology optimization shapes of the NAC and RAC25 members are similar. In addition, it can be concluded from Fig. 11c that the structural topology optimization pattern of the RAC50 specimen is identical to NAC and RAC25, but the tensile region of this member is negligibly larger than that of these two specimens. Again, although the optimization patterns of the RAC75 and RAC100 members are almost similar, it is seen in Figs. 11e-f that the compressive region of the RAC100 corbel is higher than that of the RAC75 corbel. Furthermore, it is observed from Fig. 11 that the compressive regions of both RAC75 and RAC100 specimens are higher than that of the other three specimens (NAC, RAC25, RAC50) because of the low modulus of elasticity and concrete compressive strengths. It should also be noted that the structural members are exposed to similar loading conditions; those with low concrete compressive strength and modulus of elasticity need more concrete regions to give the same response to the current load as the other specimens (NAC, RAC25, RAC50). Therefore, the concrete compressive regions of these specimens are larger than that of their counterparts. Besides, the previous studies have stated that incorporating RCA up to 35% in new concrete does not affect the behavior of both RAC and the member containing RAC. Furthermore, the critical threshold for the ratio of RCA substituted to this RAC is 50%. It should also be mentioned from Fig. 11 that the bar element numbers of the RAC25 and NAC members are similar. At the same time, the RAC50 corbel is negligibly different from these two members (Fig. 11a-c). However, RAC75 and RAC100 specimens showed completely different features from these three specimens regarding bar elements. This situation supports the presented results in the literature and reveals that the ITD method is an effective method for structural topology optimization. Finally, comparing the optimization shapes of multi-material NAC members with the multi-material RAC members indicated that the structural topology optimization process applied to single short corbels and columns incorporating NA is also valid for single short corbels and columns containing RCA. Furthermore, the structural topology optimization process of the members from initial structure to

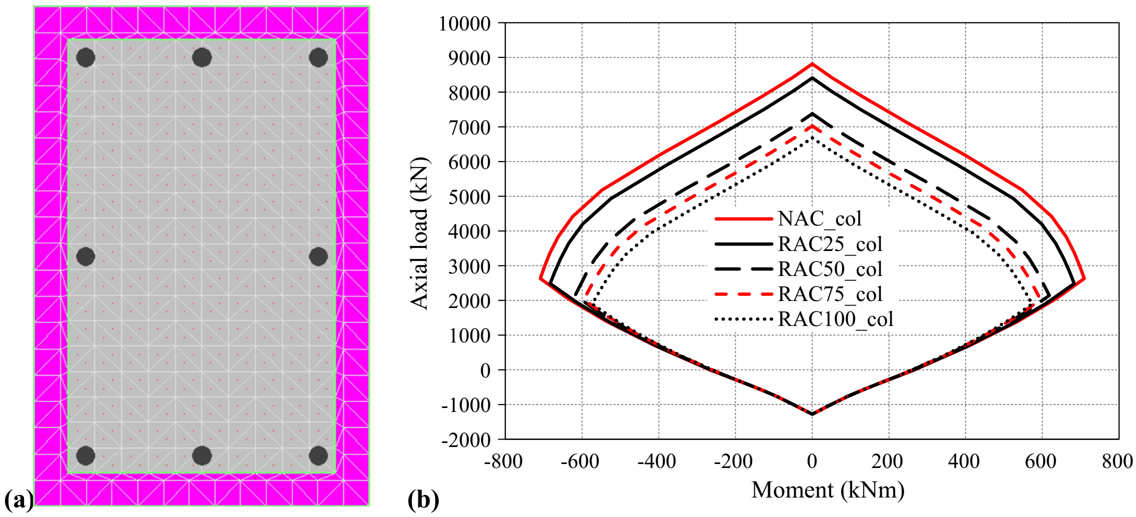

Fig. 10 Cross-sectional analysis of RC columns, **a** fibers properties, **b** axial load-moment capacities of RC columns

final optimized structure for different iterations is presented in Fig. 12.

The structural topology optimization method designs the structural members according to more than one material and loading conditions. Within the scope of this study, in addition to the analysis of RC members by considering two different materials (concrete and reinforcement) groups, an analysis of single-material (only concrete) corbels and columns containing only NAC or RAC was also conducted. The structural optimization results of these single-material structural members are given in Fig. 13. As seen in this figure, all single-material members (NAC, RAC25, RAC50, RAC75, RAC100) have the same structural optimization shapes. Therefore, it is mentioned from these results that RCA does not affect the single-material optimization process. Besides, in the single-material structural topology optimization process, the concrete performs until it is completely crushed and there is no material (such as reinforcement) to assist.

On the other hand, it has been stated in the literature that the conventional behavior (stress–strain, load–displacement, moment–curvature etc.) of NAC and RAC structural members are similar, even if the ratio of RCA in the new concrete increases. Therefore, the single-material structural members generally have the same optimization shapes since the concrete performed until crushed. Furthermore, comparing the optimization shapes of single-material NAC members with the single-material RAC members indicated that the structural topology optimization process applied to members incorporating NA is also valid for RAC members. And the structural topology optimization process from initial structure to final optimized structure for different iterations is presented in Fig. 14.

5 Life Cycle Assessment of the RCA

The ratio of construction and demolition wastes, mine and quarry wastes generated by economic activities and households in total waste is approximately 63% (Fig. 15, Table 4) [5]. About 70% of the waste consists of waste concrete or materials used in aggregate production [1–4]. Therefore, it is crucial to eliminate the construction and demolition waste concrete with environmentalist methods.

Although more than one method has been developed in recent years to eliminate the construction and demolition waste concrete, the most effective of these methods is 4R: Reduce, Reuse, Recycle, Rebuy or Resell. It has been displayed by statistical data that there are significant decreases in the amount of waste concrete originating from the construction sector of European countries that apply this method (Fig. 1).

This section of this paper provides a brief overview of RCA's life cycle assessment (LCA), which is used as aggregate in newly built structural members. Life Cycle Assessment method, which is a technique for evaluating environmental impacts of a product or process over its entire life cycle, estimates materials, energy resources, and ecological emissions activities in a sector or economy. Since the construction sector in Turkey did not have the LCA database, a similar database for Greenhouse Gases (GHGs) data and Conventional Air Pollutant (CAP) data of the construction sector for using the LCA were benefitted from the "eiolca.net" [61] database. And the Economic (E_{co}) data of the construction sector was obtained from local suppliers.

There are two ways for the life cycle of construction and demolition waste concrete. The first way is to recycle the waste concrete and reuse the recycled material as a sustainable product. The second way is to dispose of the waste

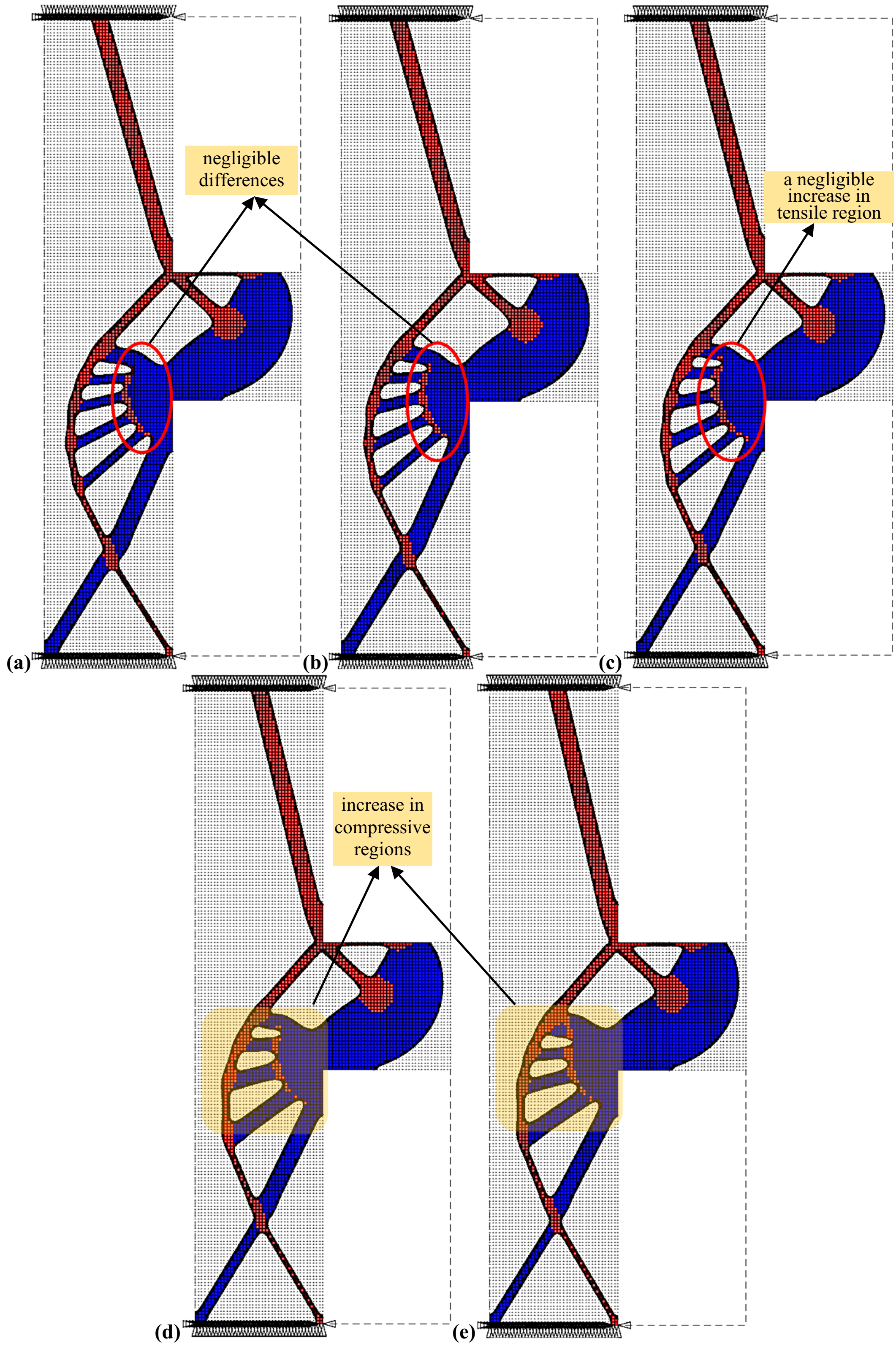

Fig. 11 Structural topology optimization shapes of the multi-material structural members obtained by performing the ITD method; **a** NAC, **b** RAC25, **c** RAC50, **d** RAC75, **e** RAC100

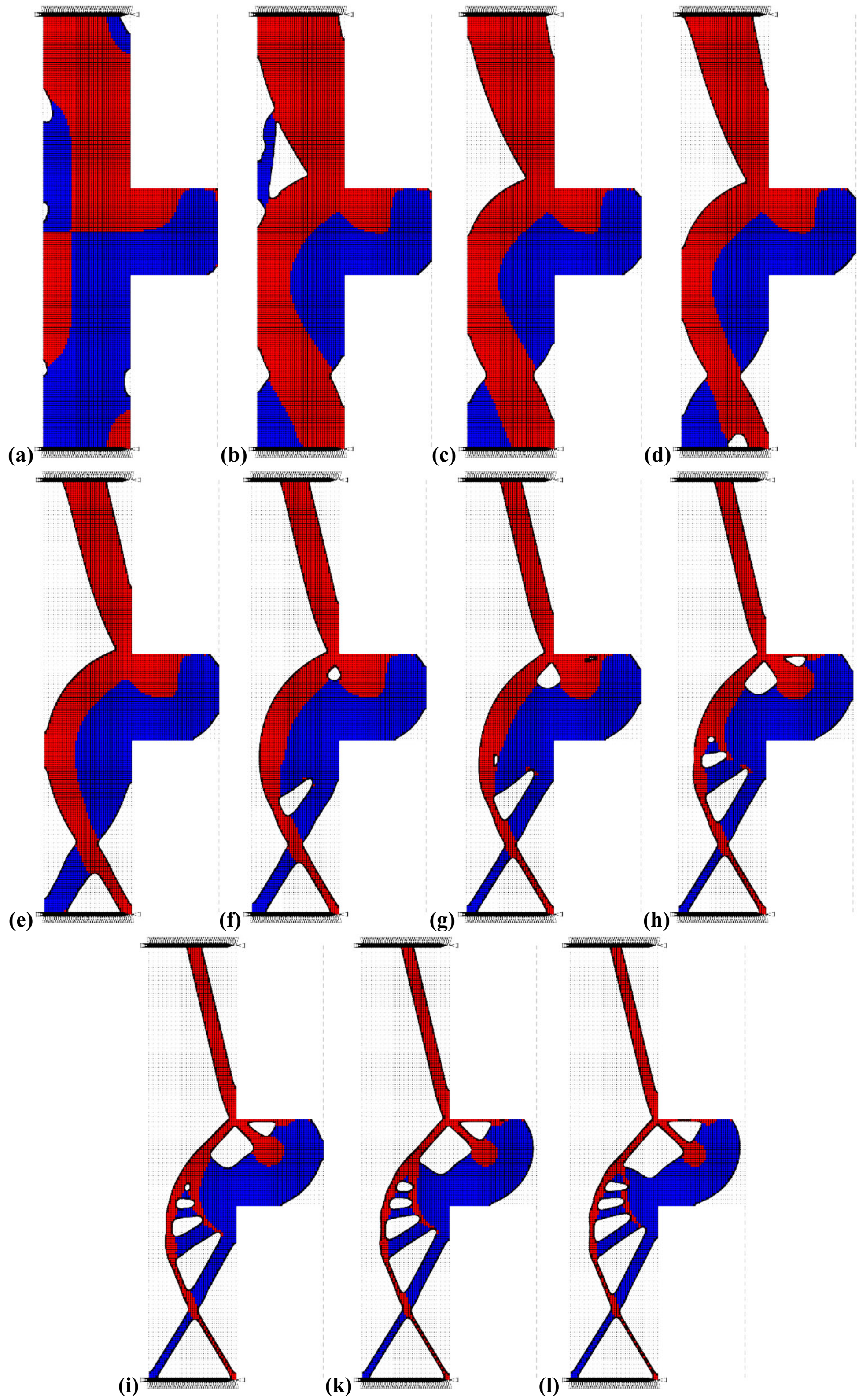

Fig. 12 Structural topology optimization process from initial to final optimized structure for different iterations; **a** 1 iteration, **b** 5 iterations, **c** 10 iterations, **d** 15 iterations, **e** 20 iterations, **f** 25 iterations, **g** 30 iterations, **h** 35 iterations, **i** 40 iterations, **k** 45 iterations, **l** final structure

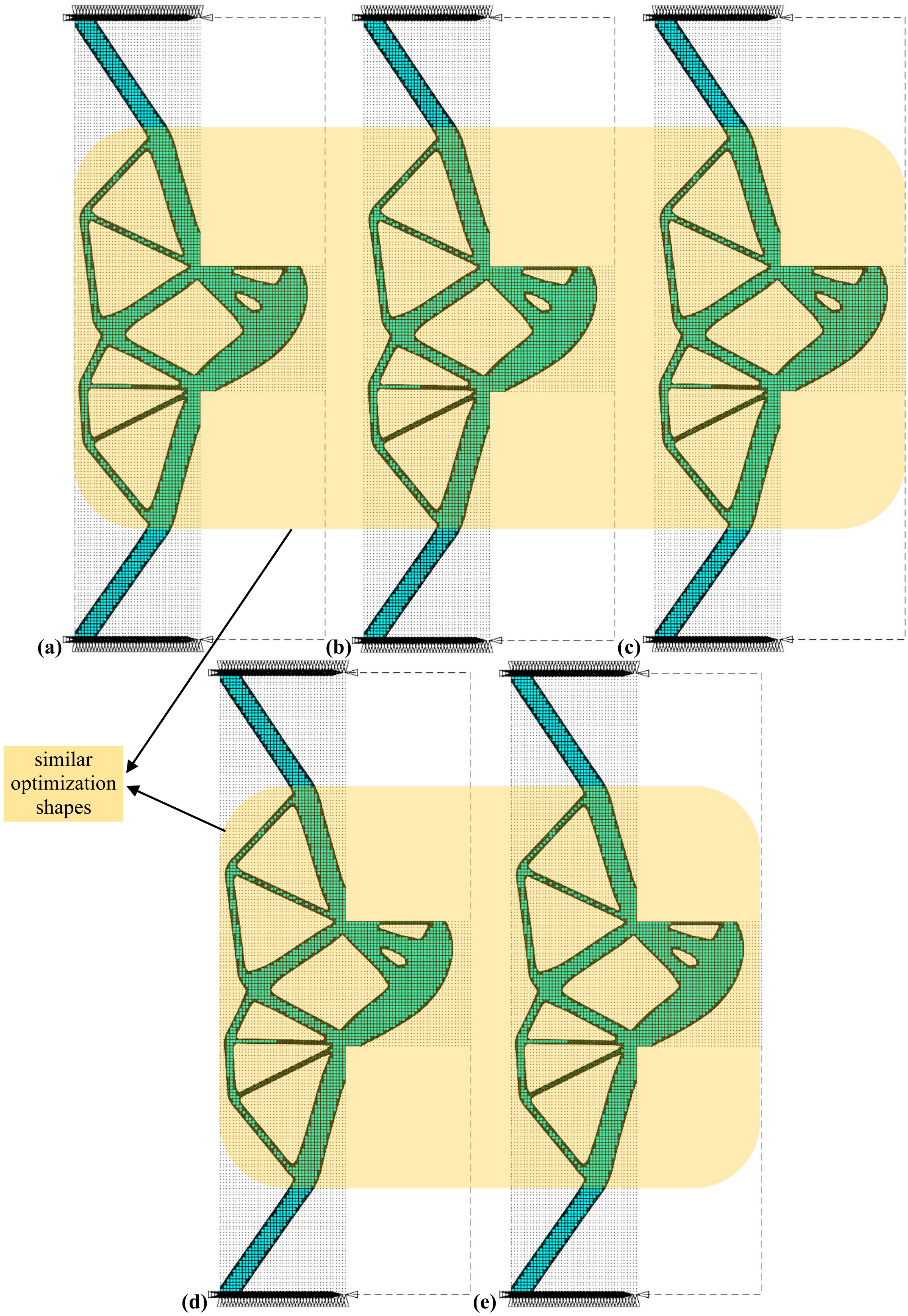

Fig. 13 Structural topology optimization shapes of the single-material structural members obtained by performing the ITD method; **a** NAC, **b** RAC25, **c** RAC50, **d** RAC75, **e** RAC100

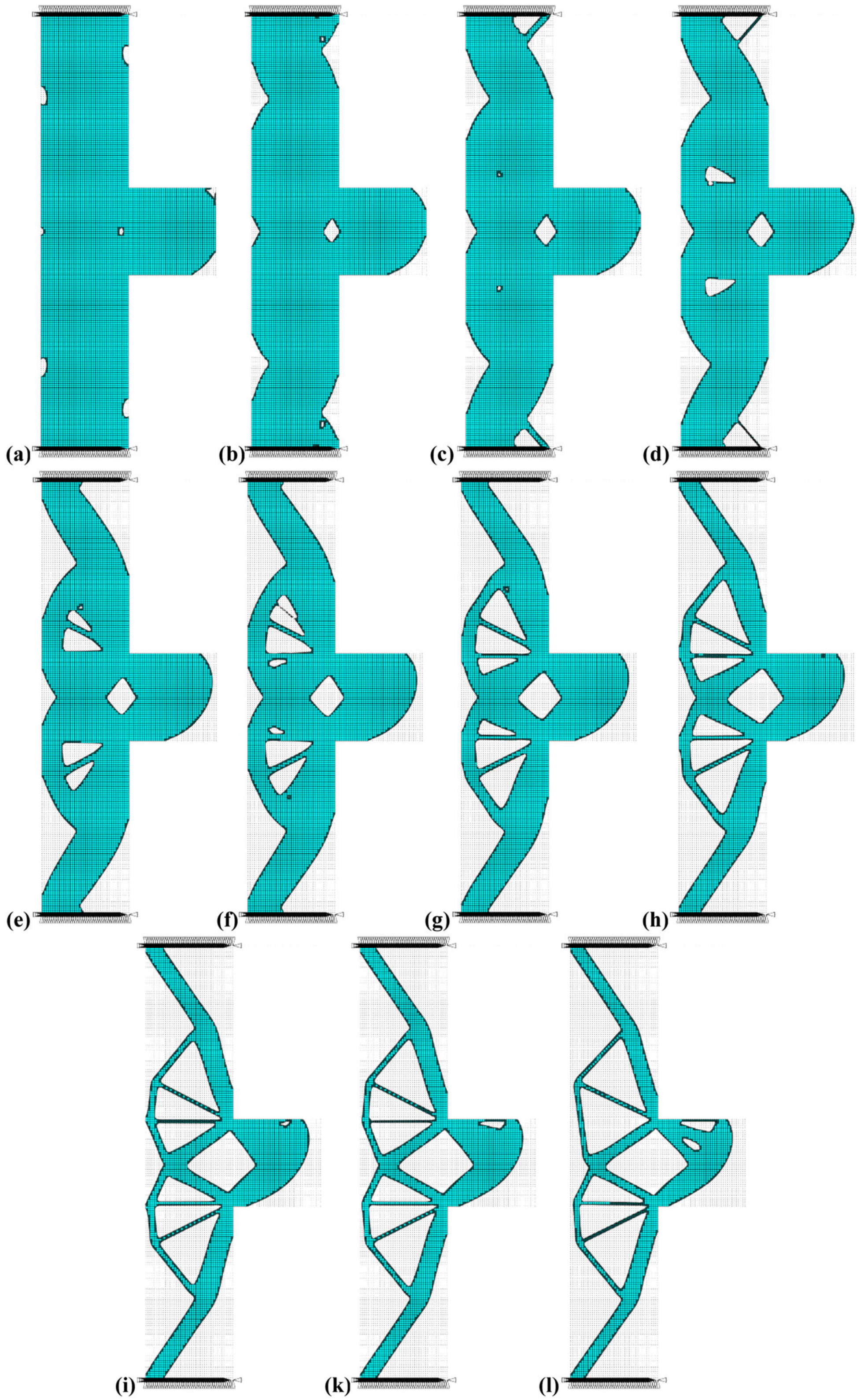

Fig. 14 Structural topology optimization process from initial to final optimized structure for different iterations; **a** 1 iteration, **b** 5 iterations, **c** 10 iterations, **d** 15 iterations, **e** 20 iterations, **f** 25 iterations, **g** 30 iterations, **h** 35 iterations, **i** 40 iterations, **k** 45 iterations, **l** final structure

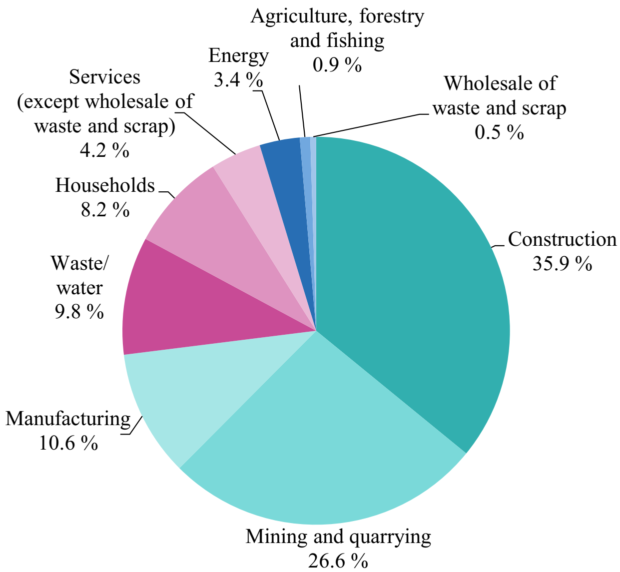

Fig. 15 Waste generation by economic activities and households (% share of total waste) [5]

concrete in the landfill area and cover the top of the waste concrete (Fig. 16).

When the construction sector chooses to recycle and reuse the waste concrete, the concrete is substantially generated by urban transformation programs; as done in the study, the industry achieves substantial economic benefit, as seen in Fig. 17. Furthermore, the first way is the significant effect on reducing Greenhouse gases and conventional air pollutant parameters in the sector (Figs. 18 and 19). On the other hand, if the industry chooses the second way, which consists of the disposal of the waste concrete to the landfill area, the method causes environmental, economic, and social problems. Even in a small-scale study conducted within the scope of this paper that unless the waste is recycled and reused as a sustainable material, the significant effects of Greenhouse gases and conventional air pollution occur in our society, as seen in Figs. 18 and 19.

6 Conclusions

This paper presents the results of an optimization study conducted on full-scale single short corbels and columns to investigate the effects of RCA on structural topology optimization behaviors. Particular attention was paid to the impacts of single-material and multi-material conditions on the characteristics of optimization behavior. The following conclusions can be drawn from the global optimization performance of the structural members:

1. The multi-material RAC25 and RAC50 members exhibited similar structural topology optimization behavior to the NAC member. The RAC75 and RAC100 members behaved differently from their counterparts. Because, as the RCA ratio in the new concrete increases (in this case, both the concrete compressive strength and the modulus of elasticity decrease), these members' structural topology optimization behavior may change under similar loading conditions.
2. The optimization results revealed that the structural topology optimization behavior of the single-material RAC members is similar to this of the NAC member.
3. The obtained structural topology optimization relationships of RAC members, optimized through the ITD method, were in good agreement with the NAC member. These results also mention that the structural topology optimization process applied to structural members incorporating NA is also valid for structural members containing RCA.
4. Furthermore, it should also be concluded from these results that the ITD method is effective for structural topology optimization of NAC and RAC structural members.
5. The LCA study, which emphasized the importance of using recycled aggregates, revealed that recycling, reducing, and reusing construction and demolition waste concrete is vital for countries' sociological and environmental conditions.

Although this study covers a wide range of research parameters, there is an obvious need for further studies to reach more general conclusions on the use of recycled aggregates sourced from concrete waste to optimize new structures.

Table 4 Waste generation by economic activities and households in EU (% share of total waste) [5]

Countries	Mining and quarrying	Manufacturing	Energy	Construction and demolition	Other economic activities	Households
EU	26.6	10.6	3.4	35.9	15.4	8.2
Belgium	0.1	24.9	1.2	33.5	33.1	7.2
Bulgaria	82.4	2.0	10.0	0.1	3.1	2.4
Czechia	0.2	14.6	1.5	41.7	26.7	15.3
Denmark	0.0	4.7	5.1	56.0	17.8	16.4
Germany	2.2	13.9	2.3	55.5	16.8	9.2
Estonia	29.5	18.8	32.3	9.5	7.6	2.4
Ireland	14.2	24.7	1.1	13.6	35.1	11.4
Greece	56.4	11.8	7.6	5.0	9.2	10.1
Spain	17.1	9.9	2.4	27.6	26.5	16.5
France	0.4	6.6	0.4	70.2	13.7	8.7
Croatia	12.0	8.9	1.3	22.7	31.7	23.3
Italy	0.8	16.5	1.3	35.3	28.7	17.5
Cyprus	6.6	16.3	0.1	45.8	14.5	16.8
Latvia	0.1	21.7	2.5	17.5	25.7	32.6
Lithuania	1.6	37.2	2.1	8.8	30.3	20.0
Luxembourg	0.0	6.9	0.1	81.2	9.7	2.1
Hungary	1.0	14.3	11.2	33.2	25.4	14.9
Malta	1.6	1.0	0.0	78.8	11.2	7.4
Netherlands	0.0	9.6	1.1	70.0	13.3	6.0
Austria	0.1	8.7	0.8	74.4	9.3	6.7
Poland	36.7	17.0	10.7	9.7	20.6	5.3
Portugal	0.2	19.0	1.1	8.8	38.1	32.8
Romania	88.0	3.9	3.4	0.3	2.4	2.1
Slovenia	0.2	20.2	11.8	8.1	51.9	7.8
Slovakia	2.2	27.5	7.9	4.4	39.8	18.2
Finland	74.9	6.7	1.0	12.3	3.5	1.6
Sweden	74.7	3.7	1.4	8.9	8.0	3.2
Iceland	0.0	24.4	0.0	3.9	31.5	40.2
Liechtenstein	1.6	1.5	0.0	88.6	1.6	6.7
Norway	1.2	12.8	1.5	40.0	27.4	17.1
Montenegro	27.4	3.7	27.6	11.3	8.6	21.4
Macedonia	14.2	46.6	0.5	3.1	35.6	0.0
Serbia	75.6	2.9	14.7	1.1	2.1	3.6
Turkey	17.9	–	26.1	0.0	7.1	28.9
Bosnia	8.2	28.1	48.1	1.8	0.2	13.6
Kosovo (1) (2)	93.5	2.0	3.4	0.1	0.0	1.0

(1) 2016, EU: European Union
(2) This designation is without prejudice to positions on status, and is in line with UNSCR 1244/1999 and the ICJ Opinion on the Kosovo Declaration of Independence

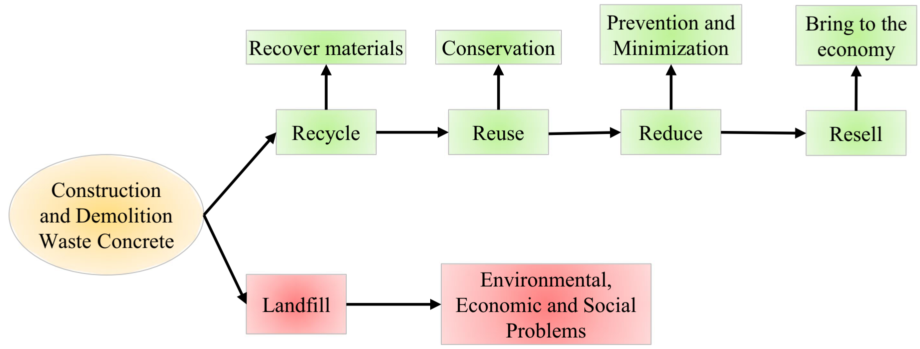

Fig. 16 Two ways for the construction and demolition of waste concrete

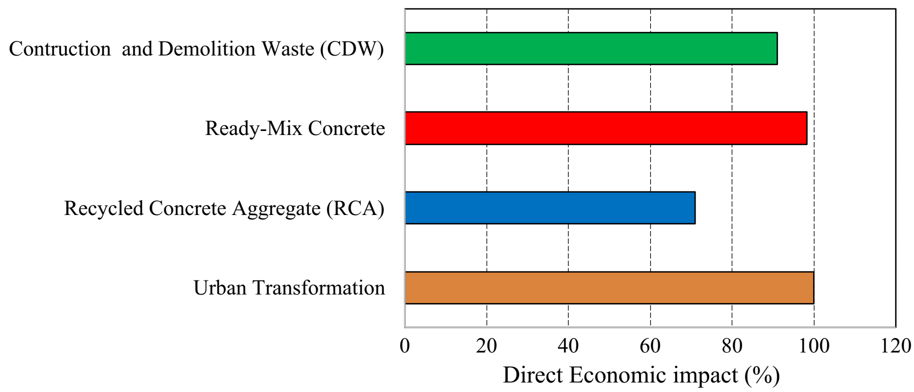

Fig. 17 The direct economic impact of the materials on LCA

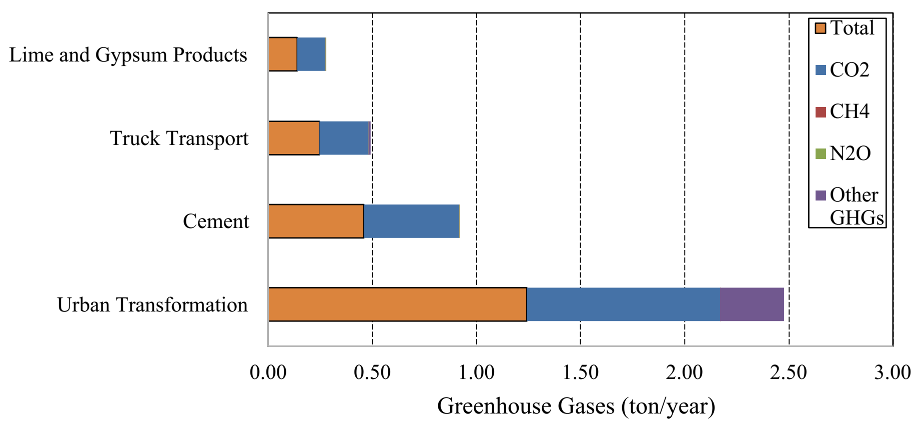

Fig. 18 The Greenhouse gases emission of the construction sector (CO_2: Carbon dioxide, CH_4: Methane, N_2O: Nitrous oxide, GHGs: Greenhouse gases)

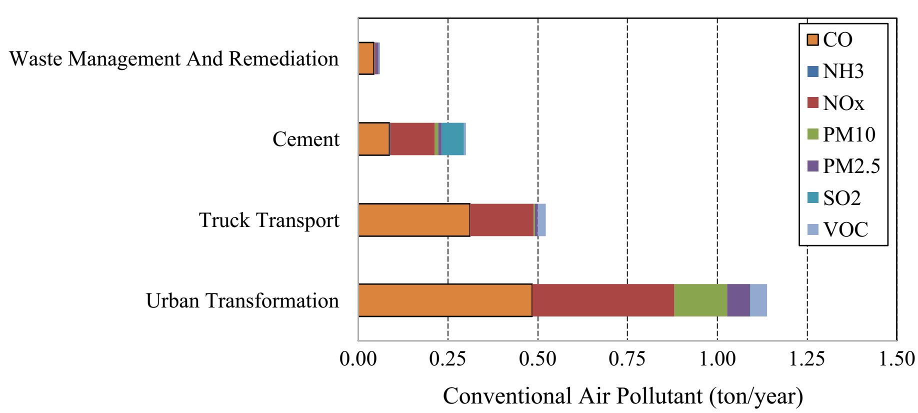

Fig. 19 The conventional air pollutant of the construction sector (CO: Carbon monoxide, NH3: Ammonia, NOx: Nitrogen oxides, PM10: Particulate matters less than 10 microns, PM2.5: Particulate matters less than 2.5 microns, SO_2: Sulfur dioxide, VOC: Volatile organic compounds)

References

1. Hansen, T.C.: Recycling of Demolished Concrete and Masonry. E&FN SPON, London (1992)
2. Khalaf, F.M.; DeVenny, A.S.: Recycling of demolished masonry rubble as coarse aggregate in concrete: review. J. Mater. Civ. Eng. **16**(4), 331–340 (2004)
3. J. Xiao, Recycled aggregate concrete structures, (2018) ISBN 978–3–662–53987–3.
4. Menegaki, M.; Damigos, D.: A review on current situation and challenges of construction and demolition waste management. Curr. Opi. Green and Sust. Che. **13**, 8–15 (2018)
5. Eurostat, Available online: https://appsso.eurostat.ec.europa.eu/nui/submitViewTableAction.do. Accessed on 19 August 2021, (updated in 30.04.2021).
6. Xie, T.; Gholampour, A.; Ozbakkaloglu, T.: Toward the development of sustainable concretes with recycled concrete aggregates: comprehensive review of studies on mechanical properties. J. Mater. Civ. Eng. **11**(1), 10–23 (2018)
7. M.C. Rao, S.M. Bhattacharyya, S.V. Barai, Systematic approach of characterization and behaviour of recycled aggregate concrete, (2019). https://doi.org/10.1007/978-981-10-6686-3
8. Goksu, C.; Saribas, I.; Binbir, E.; Akkaya, Y.; Ilki, A.: Structural behavior of recycled aggregates concrete obtained from low quality concrete. Struc. Eng. Mech. **69**(1), 77–93 (2019)
9. Saribas, I.; Goksu, C.; Binbir, E.; Ilki, A.: Seismic performance of full-scale RC columns containing high proportion recycled aggregate. Bull. Earthquake Eng. **17**(11), 6009–6037 (2019)
10. Saribas, I.; Goksu, C.; Binbir, E.; Ilki, A.: Shear-flexure interaction in RAC columns under simulated seismic actions. Eng. Struc. **231**, 111746 (2021)
11. Gonçalves, P.; De Brito, J.: Recycled aggregate concrete (RAC)-Comparative analysis of existing specifications. Mag. of Conc. Res. **62**(5), 339–346 (2010)
12. ACI 318–19: Building Code Requirements for Structural Concrete and Commentary, ACI Committee 318, (2019).
13. AASHTO LRFD: Bridge Design Specifications, Third Edition, American Association of State Highway and Transportation Officials, Washington, DC (2007).
14. CSA-S6–06: Canadian Highway Bridge Design Code, Canadian Standards Association, Mississauga, Ontario (2006).
15. Eurocode-2: Design of concrete structures - Part 1–1: General rules and rules for buildings. Standard, European committee for standardization, Brussels, (2004).
16. Saint-Venant, A.J.C.B.: Memoire sur la torsion des prismes, mem. Divers. Savants. **14**, 233–560 (1855)
17. Timoshenko, S.: History of strength of materials. McGraw-Hill, New York (1953)
18. Marti, P.: Basic tools of reinforced concrete beam design. ACI J. **82**(1), 46–56 (1985)
19. Schlaich, J.; Schafer, K.; Jennewein, M.: Toward a consistent design of structural concrete. PCI J **32**(3), 75–150 (1987)
20. Hsu, T.T.C.: Unified theory of reinforced concrete. CRC, Boca Raton (1993)
21. MacGregor, J.G.: Reinforced concrete mechanics and design, 3rd edn. Prentice-Hall, Upper Saddle River (1997)
22. Campione, G.: Performance of steel fibrous reinforced concrete corbels subjected to vertical and horizontal loads. J. Struct. Eng. **135**(5), 519–529 (2009)
23. Khosravikia, F.; Kim, H.S.; Yi, Y.; Wilson, H.; Yousefpour, H.; Hrynyk, T.; Bayrak, O.: Experimental and numerical assessment of corbels designed based on strut-and-tie provisions. J. Struct. Eng. **144**(9), 04018138 (2018)
24. W. Ritter, Die Bauweise Hennebique (The Hennebique System). Schweizerische Bauzeitung, Bd. XXXIII, 7, Zürich, (1899).
25. E. Mörsch, Der Eisenbetonbau, seine theorie und anwendung (reinforced concrete, theory and application), Stuttgart, (1902).
26. Mörsch, E.: Concrete-steel construction. Goodrich EP, McGraw-Hill, New York (1909)
27. Kupfer, H.: Generalization of Mörsch truss analogy using principle of minimum strain energy. CEB Bull. **40**, 44–57 (1964)
28. P. Lampert, B. Thürlimann, Ultimate strength and design of reinforced concrete beams in torsion and bending, Springer (1971) 107–131.
29. Collins, M.P.; Mitchell, D.: Shear and torsion design of prestressed and non-prestressed concrete beams. PCI J. **25**(5), 32–100 (1980)
30. Schlaich, J.; Schafer, K.: Design and detailing of structural concrete using strut-and-tie models. Struct. Eng. **69**(6), 113–125 (1991)
31. Liang, Q.Q.; Xie, Y.M.; Steven, G.P.: Topology optimization of strut-and-tie models in reinforced concrete structures using an evolutionary procedure. ACI Struct. J. **97**(2), 322–330 (2000)
32. Tjhin, T.N.; Kuchma, D.A.: Computer-based tools for design by the strut-and-tie method: advances and challenges. ACI Struct. J. **99**(5), 586–594 (2002)
33. Zheng, J.; Zhen, L.; Li, H.; Jiang, C.: Robust topology optimization for cellular composites with hybrid uncertainties. Int. J. Numer. Methods Eng. **115**(6), 695–713 (2018)
34. Wang, H.; Cheng, W.; Zhang, M.; Du, R.; Xiang, W.: Non-gradient Robust Topology Optimization Method Considering Loading Uncertainty. Arab. J. Sci. Eng. **46**(12), 12599–12611 (2021)
35. Ali, M.A.; White, R.N.: Automatic generation of truss model for optimal design of reinforced concrete structures. ACI Struct. J. **98**, 431–442 (2001)
36. Guan, H.: Effect of sizes and positions of web openings on strut and-tie models of deep beams. Adv. Struct. Eng. **8**(1), 69–84 (2005)
37. Leu, L.J.; Huang, C.W.; Chen, C.S.; Liao, Y.P.: Strut-and-tie design methodology for three-dimensional reinforced concrete structures. J. Struct. Eng. **132**(6), 929–938 (2006)
38. Kwak, H.G.; Noh, S.H.: Determination of strut-and-tie models using evolutionary structural optimization. Eng. Struct. **28**, 440–1449 (2006)
39. Guan, H.; Doh, J.H.: Development of strut and tie models in deep beams with web openings. Adv. Struct. Eng. **10**(6), 697–711 (2007)
40. Bruggi, M.: Generating strut and tie patterns for reinforced concrete structures using topology optimization. Comput. Struct. **87**, 1483–1495 (2009)
41. Bruggi, M.: On the automatic generation of strut and tie patterns under multiple load cases with application to the aseismic design of concrete structures. Adv. Struct. Eng. **13**(6), 1167–1181 (2010)
42. M.P. Bendsoe, Optimization of structural topology, shape and material, Springer-Verlag (1995).
43. M.P. Bendsoe, O. Sigmund, Topology optimization, Theory, methods and applications, Springer Verlag (2003).
44. G.I.N. Rozvany, T. Lewinski, Topology optimization in structural and continuum mechanics. CISM international center for mechanical sciences, Springer Wien (549) (2014).
45. O.M. Querin, M. Victoria, C. Alonso, R. Ansola, P. Marti, Topology design methods for structural optimization, Elsevier Academic Press, eBook ISBN: 9780080999890, (2017).
46. E. Hognestad, A study of combined bending and axial load in reinforced concrete members, University of Illinois Bulletin 49 no. 22 (1951).
47. Saribas, I.: Stress-strain model for recycled aggregate concretes. El-Cezerî J. Sci. Eng. **6**(1), 156–165 (2019)
48. Xiao, J.; Li, J.; Zhang, C.: Mechanical properties of recycled aggregate concrete under uniaxial loading. Cem. Concr. Res. **35**, 1187–1194 (2005)
49. Belen, G.F.; Fernando, M.A.; Diego, C.L.; Sindy, S.P.: Stress-strain relationship in axial compression for concrete using recycled saturated coarse aggregate. Constr. Build. Mater. **25**(5), 2335–2342 (2011)

50. Breccolotti, M.; Alessandro, A.D.; Roscini, F.; Bonfigli, M.F.: Investigation of stress-strain behavior of recycled aggregate concrete under cyclic loads. Environ. Eng. Manag. J. **14**(7), 1543–1552 (2015)
51. Turkish Building Earthquake Code (TBEC-18), Regulations for Buildings to be constructed in Earthquake Prone Areas, Ankara, Turkey, (2018).
52. Victoria, M.; Marti, P.; Querin, O.M.: Topology design of two-dimensional continuum structures using isolines. Comput. Struct. **87**, 101–109 (2009)
53. Victoria, M.; Querin, O.M.; Marti, P.: Topology design for multiple loading conditions of continuum structures using isolines and isosurfaces. Fin. El Anal. Des. **46**, 229–237 (2010)
54. Victoria, M.; Querin, O.M.; Marti, P.: Generation of strut-and-tie models by topology design using different material properties in tension and compression. Struct. Multidisc. Optim. **44**, 247–258 (2011)
55. O.M. Querin, M. Victoria, C. Diaz, P. Marti, Layout optimization of multi-material continuum structures with the isolines topology design method, Eng Opt (2014).
56. M. Victoria, O.M. Querin, C. Diaz, P. Marti, liteITD a MATLAB Graphical User Interface (GUI) program for topology design of continuum structures, Adv in Eng Softw 100. 126–147 (2016). (https://www.upct.es/goe/software/liteITD_i.php).
57. Dewhurst, P.: A general optimality criterion for combined strength and stiffness of dual-material-property structures. Int. J. Mech. Sci. **47**, 293–302 (2005)
58. TS 500–2000, Requirements for design and construction of reinforced concrete structures, Turkish Standards Institute, AFAD, Ankara, Turkey.
59. XTRACT 3.0.8: Cross-sectional structural analysis of components. TRC, Rancho Cordova (2007).
60. Mander, J.B.; Priestley, M.J.N.; Park, R.: Theoretical stress-strain model for confined concrete. ASCE J. Struct. Eng. **114**(8), 1804–1826 (1988)
61. http://www.eiolca.net/cgi-bin/dft/use.pl